

Supplementary information

Dehydration does not affect lipid-based hydration lubrication

Yihui Dong¹, Nir Kampf¹, Yaelle Schilt², Wei Cao³, Uri Raviv², Jacob Klein^{1*}

¹*Department of Molecular Chemistry and Materials Science, Weizmann Institute of Science, Rehovot, 76100, Israel.*

²*Institute of Chemistry, The Hebrew University of Jerusalem, Jerusalem 9190401, Israel.*

³*Department of Physical Chemistry, School of Chemistry, Tel Aviv University, Tel Aviv, 6997801, Israel.*

Content sections:

- S1. Zeta potential measurements
- S2. AFM imaging of POPC-SUV layers
- S3. Shear forces between POPC-SUV layers
- S4. X-ray scattering measurements on HSPC-SUV dispersions
 - A. The liposome model
 - B. Fitting parameters
 - C. WAXS results and analysis
- S5. Molecular dynamics simulations
- S6. Atomic force microscopy (AFM) imaging of HSPC-SUV

S1. Zeta potential measurements:

Table S1. Zeta potential measurements of HSPC-SUVs, POPC-SUVs in pure water and in 3 mol%, 6mol% DMSO.

Samples	Zeta potential, mV			
	Pure water	In pure water	In 3 mol% DMSO	In 6 mol% DMSO
HSPC-SUVs	-0.108±0.03	+4.51±0.55	+13.3±0.80	+15.6±0.58
POPC-SUVs	-0.168±0.03	-3.99±0.63	+0.724±0.36	+2.75±0.50

S2. AFM measurements of POPC-SUVs.

The morphologies of POPC-SUVs adsorbed on mica in the absence and in the presence of 3 mol% DMSO are shown in Fig. S7. No individual liposomes were seen, indicating that liposome rupture and fusion has occurred spontaneously and formed a continuous lamellar phase. Only several individual holes (or defects) were observed in the presence of 3 mol% DMSO with a thickness of roughly 2.5 nm. There was also no significant difference in the morphologies of POPC liposomes in dispersion of water or DMSO solution.

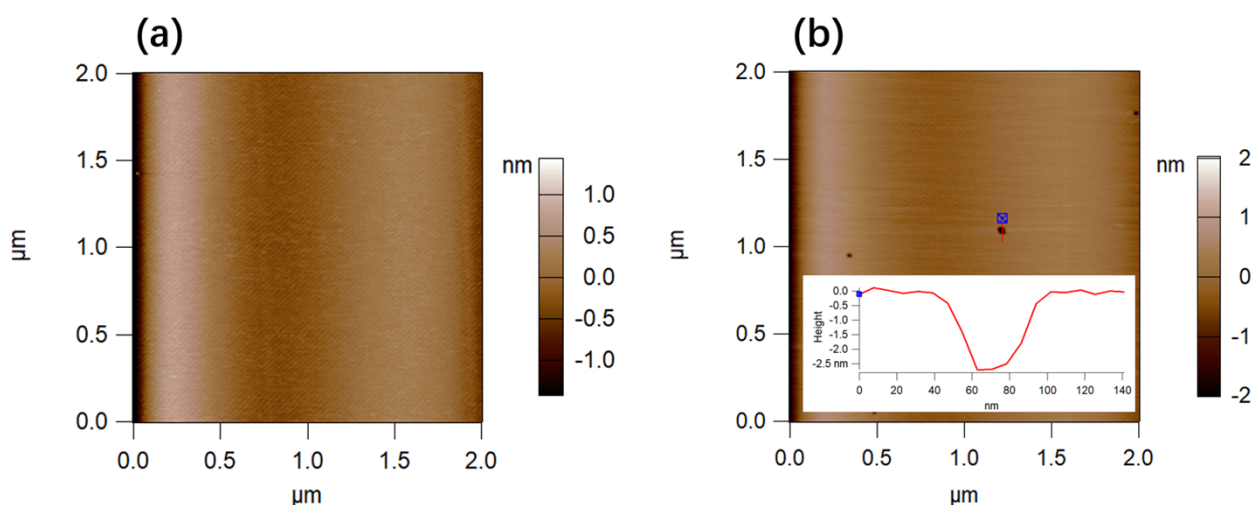


Figure S1. AFM-measured height images of POPC-SUV in dispersion of pure water(a), and 3 mol% DMSO (b). The smooth uniform layer shows the POPC bilayers formed when the SUVs ruptured. Inset: cross-section of the hole in height image, which is attributed to a defect in the upper leaflet of the bilayer.

S3. Shear force measurements with POPC layers.

Traces of the shear forces. Representative shear force traces in response to the applied lateral back-and-forth motion of the upper surface, coupled to a PZT, are shown in Fig. S6. The upper zigzag trace of each set is the applied lateral motion to the upper surface, and the traces below them show the corresponding shear forces transmitted to the lower surface under different surface separations. Very low friction forces, close to the noise level, are recorded for POPC at all the applied pressures, for both systems, even when the pressure exceeds 100 atm.

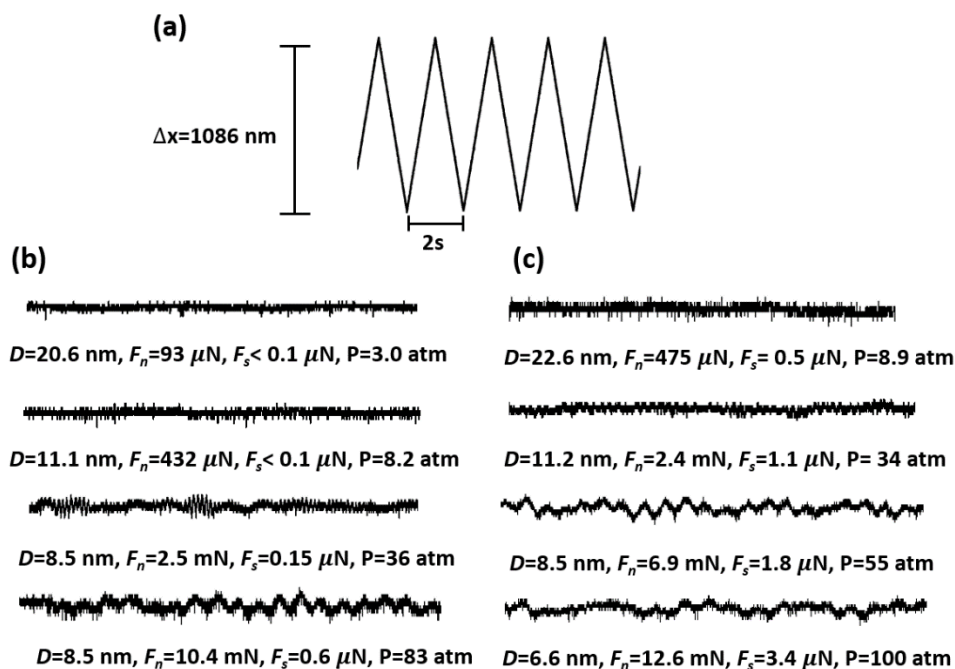


Figure S2. Typical shear force versus time traces for the POPC-SUV coated mica surface (a) across pure water (a), and 3 mol% DMSO (b).

S4. X-ray scattering measurements.

A. The liposome model

The liposome model is based on a spherical model. The inner medium of the liposome is described by a sphere with a uniform electron density contrast $\Delta\rho_{IN}$, with respect to the solvent (with electron density ρ_{out}). The membrane is composed of N multiple spherical shells where each layer has a Gaussian electron density profile along the radial direction, r . The center of the i th layer is located at r_i , its full width at half maximum (FWHM) is τ_i , and its electron density contrast, with respect to the solvent (with electron density is ρ_{out}), at r_i is $\Delta\rho_i$.

The electron density contrast of this model is:

$$\Delta\rho(r) = \Delta\rho_{IN} \cdot [\Theta(r) - \Theta(r - R_{eff})] + \sum_{i=1}^N \Delta\rho_i \cdot \exp\left[-\frac{4\ln 2 (r - r_i)^2}{\tau_i^2}\right]$$

where $R_{eff} = r_1 - \frac{\sqrt{\ln(10)/\ln(2)}}{2} \tau_1$, which is defined as the radial position where the electron density contrast of the membrane's first layer ($\Delta\rho_1$), corresponding to the inner headgroup of the lipid bilayer, is at a tenth of its maximum value.

The scattering intensity is:

$$(s1) \quad I(q) = \left[\frac{4\pi}{q^2} \Delta\rho_{IN} \left[\frac{\sin(qR_{eff})}{q} - R_{eff} \cos(qR_{eff}) \right] + \left(\rho_1 - \rho_{IN} \right) \tau_1 e^{-\frac{\tau_1^2 q^2}{16 \ln 2}} \left[m_1 + \int_0^1 \left(g_1 \times \exp\left(\frac{\tau_1^2 q^2}{16 \ln 2} - \frac{4 \ln 2 r_1^2}{\tau_1^2} \right) y^2 \right) dy \right] + \sum_{i=2}^N \Delta\rho_i \tau_i e^{-\frac{\tau_i^2 q^2}{16 \ln 2}} \left[m_i + \int_0^1 \left(g_i \times \exp\left(\frac{\tau_i^2 q^2}{16 \ln 2} - \frac{4 \ln 2 r_i^2}{\tau_i^2} \right) y^2 \right) dy \right] \right]^2$$

where y is an integration variable, m_i is:

$$m_i = -\frac{2r_i \sin(qr_i)}{\sqrt{\ln 2}} - \frac{\tau_i^2 q \cos(r_i q)}{4 \ln 2 \sqrt{\ln 2}}$$

and g_i is:

$$g_i = \left(\frac{4r_i^2}{\tau_i} - \frac{\tau_i^3 q^2}{16 \ln^2 2} \right) \sin\left[r_i q (y^2 - 1) \right] - \frac{r_i \tau_i q}{\ln 2} \cos\left[r_i q (y^2 - 1) \right].$$

Detailed derivation can be found in ¹.

B. Fitting parameters

The layers 1 and 5 correspondent to the hydrophilic parts of the membrane (head 1 and head 2). The hydrophobic part is separated in two parts as the electron density of the extremity of the PC lipid (CH_3) is different from the rest of the tail (CH_2) values of the best fitted model parameters were obtained by comparing the SAXS data with the calculated intensity of the "liposomal model" (Equation S1) for the liposomes dispersed in different DMSO / water ratio.

In the following table S2, r_0 is the radius of the liposome at the central part of the membrane, while $r_i - r_0$ is the width of the i th layer.

Table S2

		Head 1 (in) i = 1	Tails 1 (CH ₂) i = 2	Tails (CH ₃) i = 3	Tails 2 (CH ₂) i = 4	Head 2 (out) i=5	ρ_{IN} [e/nm ³]	r_0 [nm]	ρ_{OUT} [e/nm ³]	Head to Head thickness [nm]
Water	$r_i - r_0$ [nm]	-2.52	-1.53	0	1.53	1.95	333	30 ±1.5	333	4.47
	ρ_i [e/nm ³]	480.5 ± 0.5	328.24± 0.5	253.66± 0.5	328.24± 0.5	462.89± 0.5				
	τ_i [nm]	1.17	1.08	1.76	1.08	1.02				
Water + 3mol% DMSO	$r_i - r_0$ [nm]]	-2.5	-1.53	0	1.53	2	333	27±1	336	4.50
	ρ_i [e/nm ³]	476.6 7± 0.5	328.24± 0.5	253.66± 0.5	328.24± 0.5	461.83± 0.5				
	τ_i [nm]	1.142	1.083	1.758	1.083	1.039				
Water + 6mol% DMSO	$r_i - r_0$ [nm]	-2.35	-1.53	0	1.53	2.43	338± 0.5	27±1	340	4.78
	ρ_i [e/nm ³]	468.1 2± 0.5	328.24± 0.5	253.66± 0.5	328.24± 0.5	468.00± 0.5				
	τ_i [nm]	1.09	1.08	1.76	1.08	1.09				

C. WAXS results and Analysis

WAXS measurements (Figure S3) revealed the center of the tail-tail correlation peaks, q_0 . Assuming the lipid tails are arranged in a 2D hexagonal lattice the area per lipid, A , can be estimated, using²

$$A \approx 2 \cdot 1.32 \left(\frac{9\pi}{4q_0} \right)^2$$

The area per HSPC lipid in water was 0.584 and decreased to 0.579 nm² in 3 mol% DMSO. In the case of HSPC in 6 mol% DMSO, the solvent and lipid tail peaks could not be separated hence background subtraction was not applicable and the area per lipid was not determined.

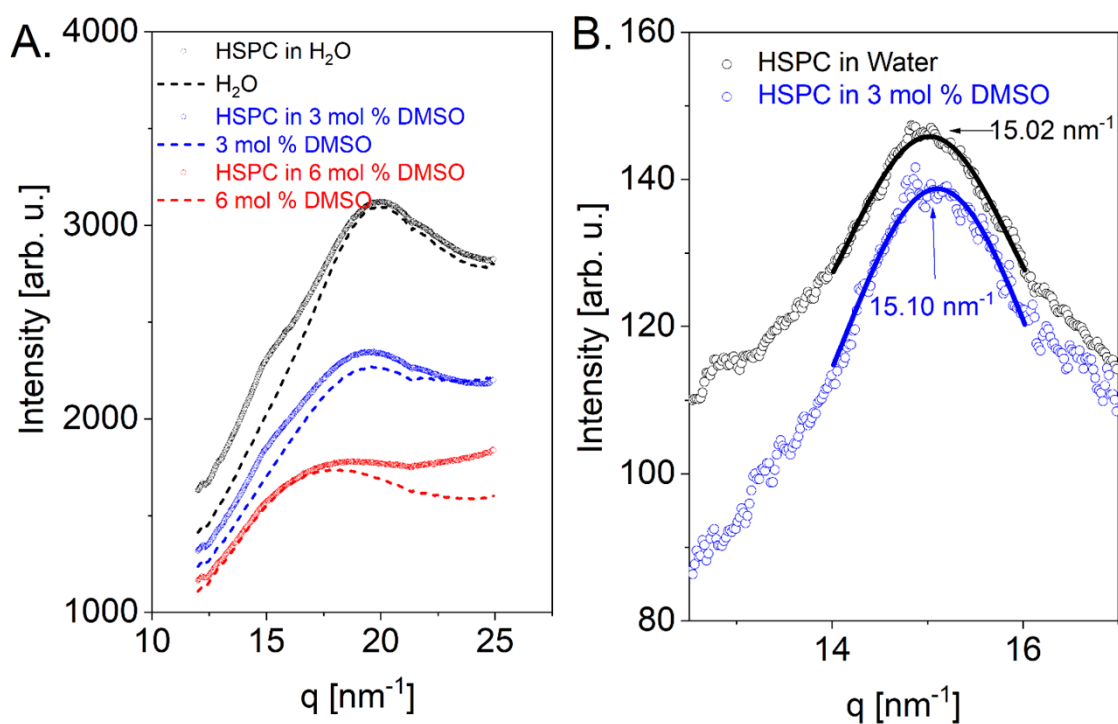


Figure S3. Wide-angle X-ray scattering (WAXS) analysis. (A.) Azimuthally-averaged WAXS intensity curves from HSPC dispersions in water, 3 mol% DMSO, and 6 mol% DMSO (solid symbols), and from pure water, 3 mol% DMSO, and 6 mol% DMSO as background. (B.) The HSPC lipid-tail correlation peaks, following background subtraction, for HSPC in water and HSPC in 3 mol% DMSO (solid symbols) are shown on an expanded scale, after baseline subtraction. The indicated peaks centers were determined by fitting to Gaussian line-shapes (solid curves).

S5. Molecular dynamics simulations.

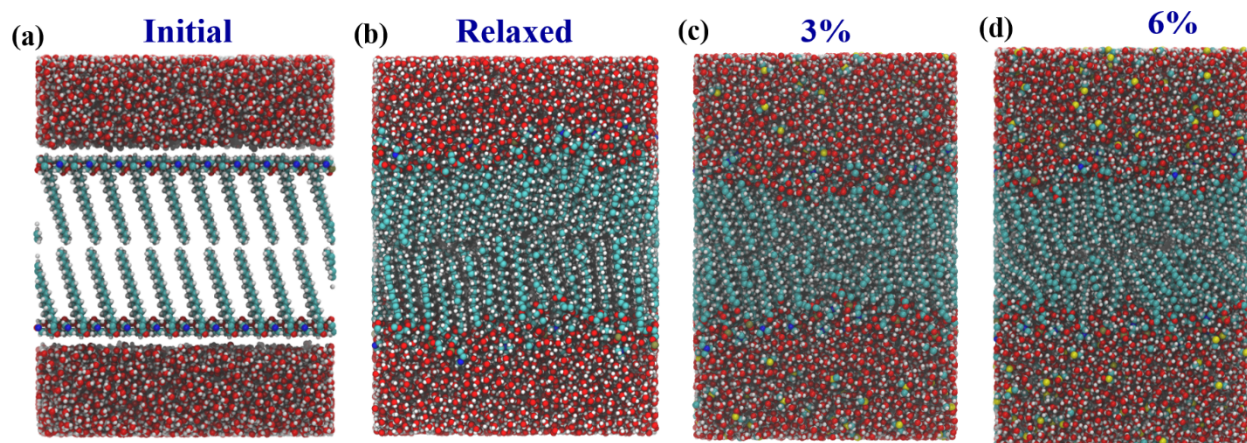


Figure S4. Snapshots of the initial simulation model of HSPC lipids (a) and after relaxation (b) in pure water. (c) and (d): Snapshots of the structures following relaxation for 3 mol% and 6 mol% DMSO, respectively.

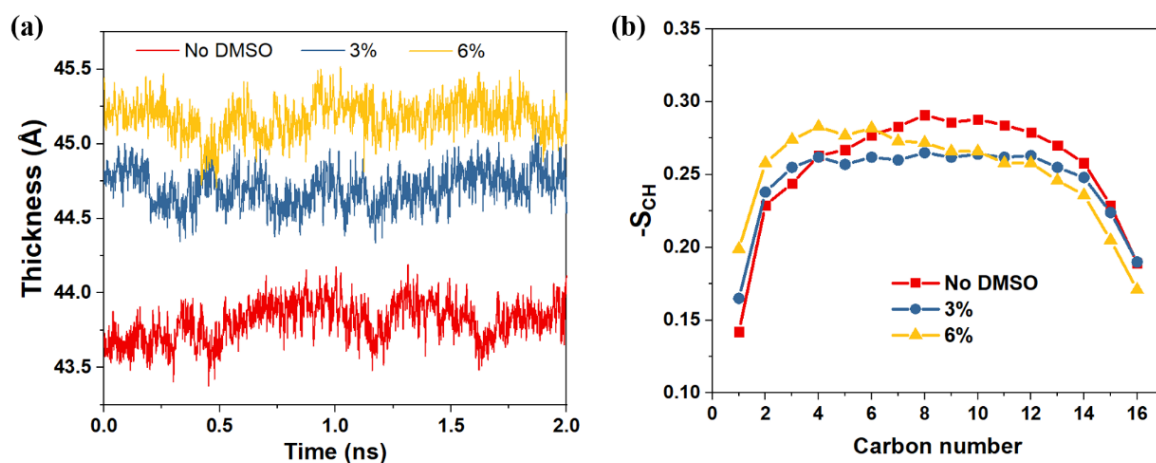


Figure S5. (a) Thickness dependence during equilibrium in the simulations. (b) Order parameter, $-S_{CH}$, for *sn*-2 chain of the HSPC lipid bilayer.

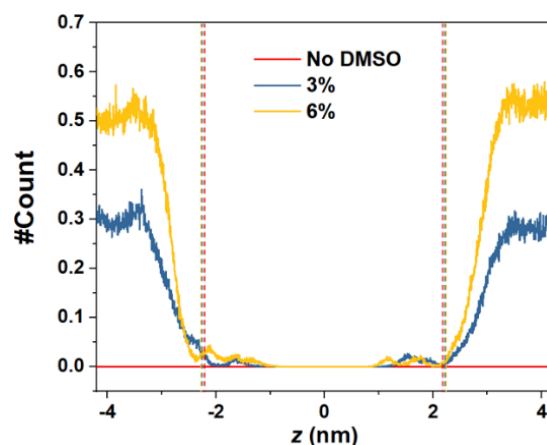


Figure S6. DMSO number density profile along the normal direction. The dashed lines mark the time averaged edge of the lipid head groups.

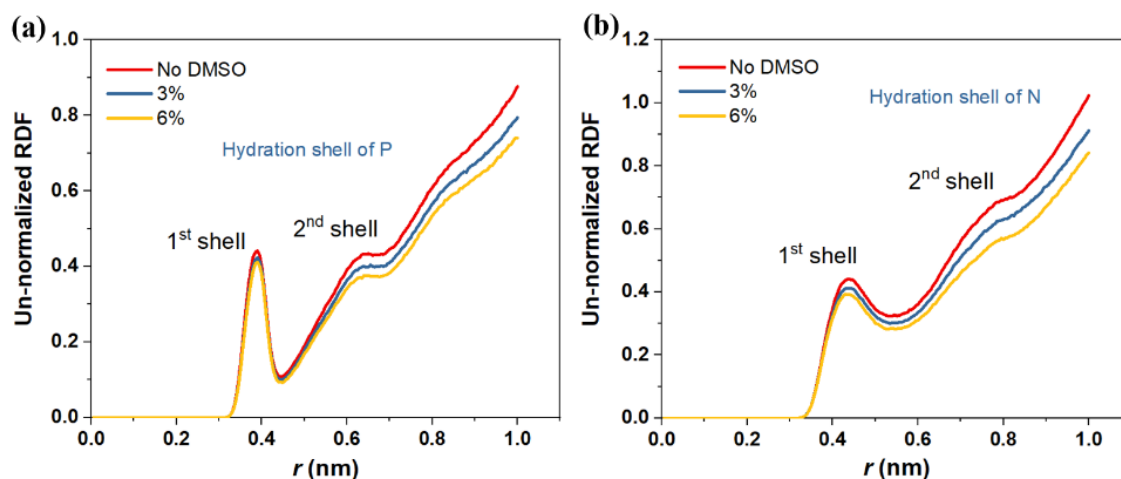


Figure S7. Un-normalized radial density function (RDF) of (a) P and (b) N atoms in lipids.

S6. Atomic force microscopy (AFM) measurements on HSPC-SUVs.

Imaging and the Young's modulus of the surfaces were carried out with an MFP-3D AFM (Oxford Instruments, Asylum Research, Santa Barbara, CA, USA) using a silicon tips on a silicon nitride lever (SNL, Bruker). Non-contact mode was used for topographical imaging and was made at room temperature. The nanomechanical mapping was obtained by the AM-FM (amplitude modulation-frequency modulation) mode using the resonance of the second cantilever Eigen mode to quantify the elastic moduli of the adsorbed liposomes. The samples were prepared by adding 20 mL 0.3 mM liposomes dispersions to a Petri dish with a cleaved mica sheet glued on the surfaces and incubated for 12 hours. These samples were used as a control (liposome dispersion, no DMSO added).

Subsequently, pure DMSO (>99.99%) solution was added to the liposomes dispersion to achieve 6 % mole fraction DMSO-water solution and then equilibrate for 2 hours. This sample was then scanned as described above.

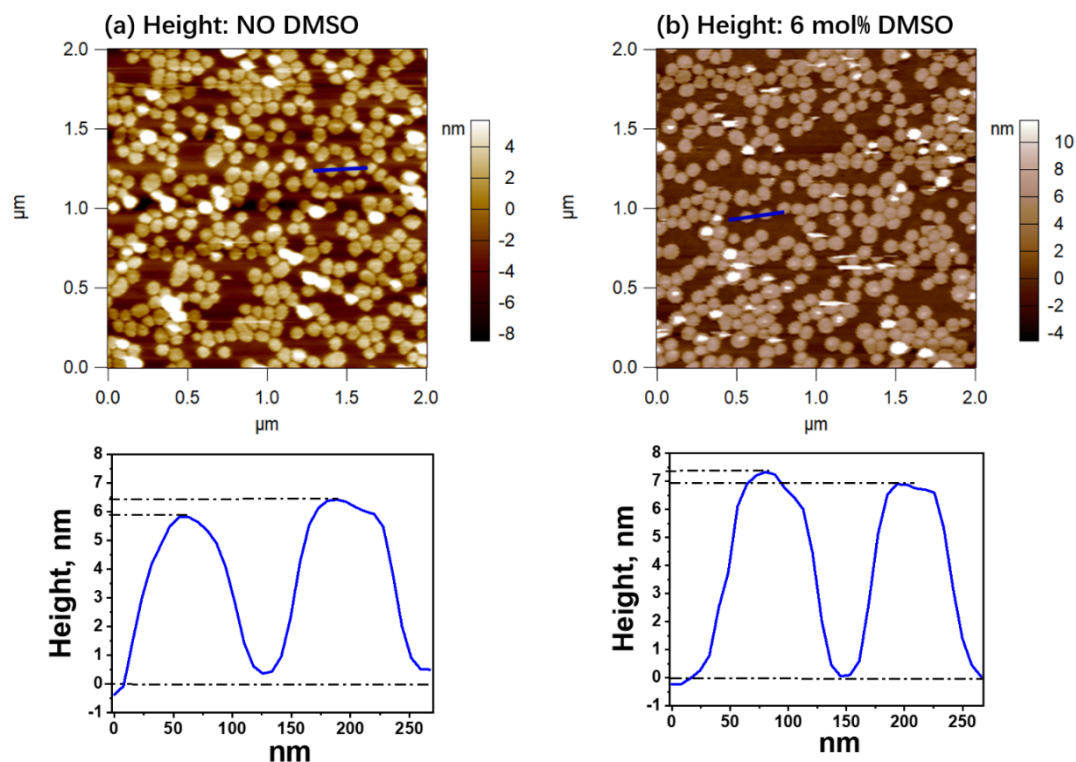


Figure S8. AFM images of HSPC-SUV adsorbed on freshly cleaved mica (a) without and (b) with 6 mol% DMSO solution. The apparent heights of the vesicles appear much less than the DLS-determined size of ca. 70 nm, an effect attributed to compression by the AFM tip during scanning (see discussion in ref. 3).³

References.

1. Székely, P.; Ginsburg, A.; Ben-Nun, T.; Raviv, U., Solution X-ray Scattering Form Factors of Supramolecular Self-Assembled Structures. *Langmuir* **2010**, *26* (16), 13110-13129.
2. Mills, T. T.; Toombes, G. E. S.; Tristram-Nagle, S.; Smilgies, D.-M.; Feigenson, G. W.; Nagle, J. F., Order Parameters and Areas in Fluid-Phase Oriented Lipid Membranes Using Wide Angle X-Ray Scattering. *Biophysical Journal* **2008**, *95* (2), 669-681.
3. Sorkin, R.; Dror, Y.; Kampf, N.; Klein, J., Mechanical Stability and Lubrication by Phosphatidylcholine Boundary Layers in the Vesicular and in the Extended Lamellar Phases. *Langmuir : the ACS journal of surfaces and colloids* **2014**, *30* (17), 5005-5014.